Growth and Optical Properties of $Li_2B_4O_7$ Single Crystals Pure and Doped with Yb, Co and Mn Ions for Nonlinear Applications

D. Podgórska[a,*], S.M. Kaczmarek[a], W. Drozdowski[b],
M. Berkowski[a] and A. Worsztynowicz[a]

[a]Institute of Physics, Technical University of Szczecin
48 Piastów Str., 70-310 Szczecin, Poland
[b]Institute of Physics, N. Copernicus University
5 Grudziądzka Str., 87-100 Toruń, Poland

The paper reports on the growth conditions of $Li_2B_4O_7$ single crystals in both pure and Yb, Co, Mn doped systems. The crystals were grown by the Czochralski method using an intentional concentration of the above--mentioned ions at a level of 0.5 mol.%. The pure and Mn-doped crystals were found to be highly transparent and clear. The crystals doped with Yb_2O_3 had a lot of precipitations making them opaque. The Co-doped crystals were purple-blue in colour and highly transparent. The growth of Yb and Co doped $Li_2B_4O_7$ crystals was reported for the first time in this paper. Absorption was measured in the range of 200 to 3200 nm, moreover analysis of changes in the absorption spectrum of γ-irradiated pure and doped $Li_2B_4O_7$ crystals was performed. Some thermoluminescence properties were measured, e.g. energies and lifetimes of the traps of different charge carriers occurring in the crystals at low temperatures.

PACS numbers: 42.25.Bs, 42.70.Mp, 81.10.Fq

1. Introduction

$Li_2B_4O_7$ (LBO) crystal is a negative uniaxial crystal, which belongs to the 4 mm point group and $I4_1cd$ (C_{4v}^{12}) space group of tetragonal symmetry ($a = b = 9.479$ Å, $c = 10.286$ Å). The crystal is uniaxial and optically negative. Its structure

---

*corresponding author; e-mail: dana@ps.pl

is determined by the B_4O_9 network with the Li^+ ions localized in the special sites in this network. B–O distance equals 1.45 Å, O–O distance equals 2.38 Å, and Li–O distance equals 2.1 Å [1].

LBO melts congruently at 1190 K at a composition of 1:2 of Li_2O and B_2O_3, so it may be grown by Czochralski [1] and Bridgman [2] methods. Rare earth and transition metal ions may substitute for both octahedral Li^+ and tetrahedral B^{3+} sites. It is expected that primarily the Li site should be occupied by all the dopant ions due to the extremely small size of the boron ion (0.23 Å). The low symmetry at the Li^+ site in LBO crystals does not offer an easy image of a distorted octahedron based on non-oxygen ions, but the number of nearest oxygen ions with the Li–O distance < 0.3 nm is 7 with four oxygens at around 0.21 nm, which is not far from the situation in an octahedral coordination.

LBO is a piezoelectric material and has been studied as a substrate for surface acoustic wave (SAW) devices [3]. Microwave devices using surface acoustic waves are in common use for infrared filters for colour television and under signal processing elements. LBO is also considered to be one of the useful materials for neutron detection because it contains Li and B, which possess large neutron capture cross-section isotopes [4].

LBO crystals have certain features in common, for example, its luminescence can be excited effectively by photons with energy in the vicinity of the long wavelength fundamental absorption edge, by roentgen or corpuscular radiation, and also through the recombination processes with the participation of the lattice defects [5]. The origin of the luminescence is attributed either to the radiative annihilation of self-trapped excitons. This spectrum represents a complex broad band in the spectral range of 250–500 nm with a maximum intensity at about 312–417 nm. Two principal Gaussians can fit it: G_1 — 234 nm and G_2 — 380 nm. It is notable that precisely the same bands appear in spectra of thermally stimulated luminescence of the doped LBO crystals. The radiation induced effects and defects in LBO crystals were examined in Refs. [4–6].

So far LBO has not been used as a primary laser host or gain medium. This is because of the tight packing of the LBO single crystal lattice and the relatively large sizes of the dopant ions. This is a reason for which mainly transition metal ions (with the atomic radii smaller than rare-earth ones) are used as active dopants. The incorporation of Ni, Cu, and Ti ions into LBO crystal was performed by Senguttuvan et al. [7]. Among other transition metal ions the divalent manganese is very often used in phosphors because of its broad emission, related to the crystal field transition $^4T_1$–$^6A_1$ in cubic symmetry [8]. Manganese was incorporated to LBO crystal for the first time by Kang-Soo Park et al. [9]. The site symmetry strongly influences the emission spectra of Mn^{2+} ions [10]. Thus, depending on the host matrix, a variety of emission colours can be obtained [10–13]. However, because of the low oscillator strength of its $d-d$ absorption transitions, crystals are usually co-activated with donor ions in order to excite the emitting Mn^{2+} ions

by energy transfer in a more efficient way. One of the possible ways is co-doping of a crystal with Eu^{2+}.

LBO single crystals doped with Co, Yb, Mn seem to be promising thermoluminescent materials because of its low phonon energy dependence [14], a radiation proof material for optical devices and a tissue-equivalent material for radiation dosimeters [15].

The influence of impurities on properties of the lithium tetraborates has not been investigated clearly enough to date. It was found that silver impurities increase the G_2 subband, whereas copper impurities drastically increase the G_1 subband of steady-state luminescence. In paper [16] a dependence of the electro-optical coefficient on the type and concentration of the dopant was revealed. An increase in the potassium concentration leads to a decrease in the electrooptical coefficient, while the increasing of the silver concentration causes just the opposite effect.

In the present investigation, we report preliminary studies on the possibility of growing of LBO single crystals with different dopants and characterizing them for optical properties. We tried to grow pure and Mn, Yb, and Co doped lithium tetraborate single crystals. The Yb, Co doping of LBO crystal was reported for the first time in this paper. We have performed the absorption, additional absorption after γ-irradiation, thermoluminescence and radioluminescence measurements to determine the defect structure of the crystals.

2. Experimental

$Li_2B_4O_7$ single crystals were grown by the Czochralski method in the Institute of Physics, Technical University of Szczecin, Poland (see Fig. 1).

The melt was prepared by melting at first B_2O_3 of 4N purity in a platinum crucible and gradually adding Li_2CO_3 of 5N purity to reach a starting composition with 67.9 mol.% of B_2O_3. The excess of B_2O_3 over the stoichiometric composition was needed because of its high vapour pressure at the crystallization temperature. The growth processes were carried out using the crucible of 50 mm in diameter and passive after a heater placed on a ceramic distance plate very close to the crucible. The first growth process was carried out using platinum wire. Seeds with orientation parallel to $\langle 110 \rangle$ direction were cut from this crystal. Following growth processes were carried out with the seed rotation rate of 5 rpm. The crystals thus obtained were transparent, colourless, without a core and with thin visible inclusions line at the centre along the crystals. The crystals' cross-sections were circular, approximately 20 mm in diameter, with two $\langle 110 \rangle$ type and two $\langle 001 \rangle$ type lines on the surface.

Optical transmittance in the wavelength region of 200–3200 nm was measured for all the samples before and after γ-irradiation using a Perkin–Elmer LAMBDA-900 Spektrofotometr in the Military University of Technology Institute of Optoelectronics, Warsaw.
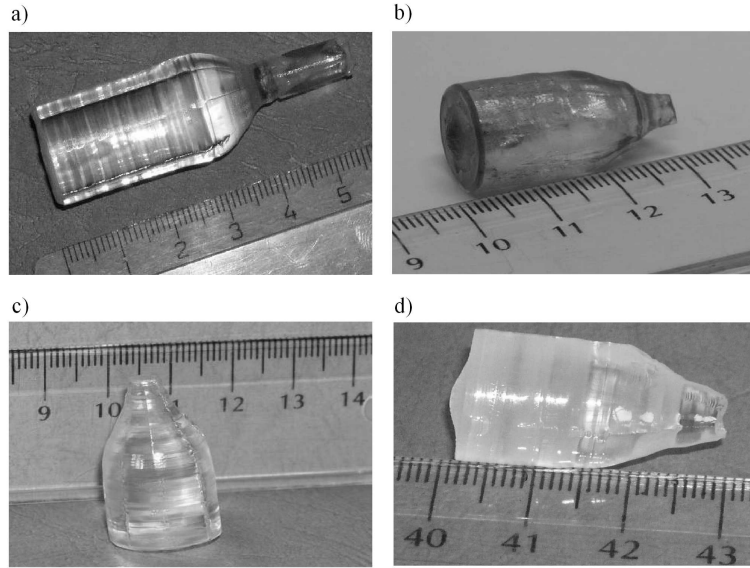
Fig. 1. Single crystals of $Li_2B_4O_7$ obtained by Czochralski method in the Institute of Physics, TU of Szczecin; (a) pure LBO single crystal, (b) LBO:Co single crystal, (c) LBO:Mn, (d) LBO:Yb single crystals.

Values of the additional absorption, $\Delta K(\lambda)$, due to the irradiation were calculated according to the formula [10]:

$$\Delta K(\lambda) = \frac{1}{d} \ln \frac{T_1}{T_2},\qquad(1)$$

where K is the absorption, $\Delta K(\lambda)$ is the additional absorption, λ is the wavelength, d is the sample thickness, and T_1 and T_2 are the transmissions of the sample measured before and after the irradiation, respectively.

Radioluminescence (RL) and low temperature thermoluminescence (TL) measurements were performed using a standard set-up consisting of an X-ray tube (DRON) operated at 42 kV and 10 mA, and a spectrograph (SpectraPro-500i made by Acton Research) equipped with a holographic grating (Hol-UV grating, 0th order, 2 mm slits), and a photomultiplier, PMT: Hamamatsu R928 (1000 V) for detection. The glow curves were recorded between 10 and 310 K at the heating rate of (0.148 ± 0.001) K/s. Before the TL runs the samples were exposed to X-ray irradiation (DRON, 42 kV/10 mA, 10 min), IF UMK Toruń.

3. Results and discussion

All the crystals were grown by the Czochralski method using an intentional concentration of the above-mentioned ions at a level of 0.5 wt.%. The pure and Mn-doped crystals were found to be colourless, highly transparent, and clear. The

Co-doped crystals were purple-blue in colour, transparent, and clear. The crystals grown with Yb_2O_3 had a lot of precipitations decreasing crystals transparency indicating the difficulties in embedding these elements in the LBO matrix.

The absorption was measured in the range from 200 nm to 3200 nm (see Fig. 2). It should be noted that the short wavelength cut-off for pure LBO is 167 nm. But crystals doped with Mn and Co showed short wavelength cut-off at about 190 nm. Mainly Co-doped crystal reveals clear absorption bands.
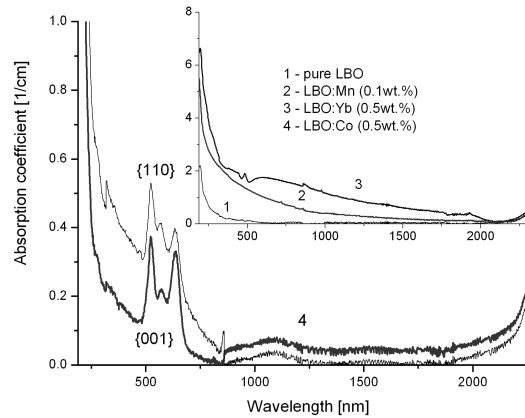

Fig. 2. The absorption of pure LBO (1), LBO:Mn (2), LBO:Yb (3) and polarized absorption of LBO:Co (4) crystals.

The main features of the absorption polarised LBO:Co spectra presented in Fig. 2 (curves No. 4) consist of some octahedral coordinated, Co^{2+} related absorption bands seen as a triple band in the visible region ($^4T_1(F) - {}^4T_1(P)$ single electronic spin-allowed transition — near 500 nm), and a small bump related to double-electronic spin-allowed $^4T_1 - {}^4A_2$ transition (near 1100 nm).

No Yb^{3+} absorption is present in the absorption spectrum of LBO:Yb single crystal but 198, 234, and 280 nm bands seen in the absorption spectrum of "as--grown" LBO:Yb crystals suggest Yb^{2+} substituting.

Some absorption bands are observed in the LBO:Mn crystals but only under influence of γ-ray irradiation.

Mn^{2+} ion gives a rise to transition between crystal field energy levels within its $3d^5$ electronic configurations. Mn^{2+} has the free ion ground state, ^6S, the only spin sextet state, and an octahedral crystal field does not split it. In an octahedral environment, in a weak crystal field ^6S transforms into $^6A_1(S)$ as the ground state, whereas ^4G splits into $^4T_1(G)$, $^4T_2(G)$, $^4E(G)$, $^4A_1(G)$. The absorption transitions are spin and parity forbidden in an octahedral environment. As a result, the absorption bands, especially for low-doped crystals, are very weak and the optical transitions of moderately Mn^{2+} doped crystals must be generally investigated by photoluminescence (excitation and emission technique).
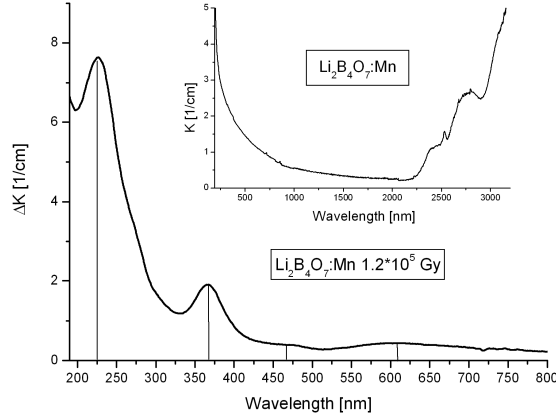
Fig. 3. Additional absorption spectrum of LBO:Mn single crystal induced by γ-ray irradiation with a dose of 1.2×10^5 Gy; in the inset the absorption spectrum of the "as-grown" crystal is presented.

The absorption spectrum of "as-grown" $Li_2B_4O_7$:Mn single crystal (see the inset to Fig. 3) does not reveal the presence of clear Mn^{2+} absorption band, but the induced absorption spectrum, shown in Fig. 3, reveals the presence of several bands peaked at: 225, 370, 470, and 610 nm. The 470 nm band we assigned to Mn^{2+} absorption, 610 nm is probably attributed to Mn^{5+} or F^{2+} colour centre absorption, while 225 and 370 nm bands are connected with higher valence states of manganese [8]. We can assign the former to Mn^0B centre (Mn^0 substituting for Li^+ in off-centre position; Mn^0 is formed as a result of the Compton electron capture by Mn^{1+} ion), and, the latter to $Mn^{6+}(d^1)$. There is observed also a weak broad absorption band with a maximum at about 800 nm (usually attributed to Mn^{6+} (T_d) $^2E - ^2T_2$ ligand-field transition).

It means the ions being recharged by γ-rays were substituted also for tetrahedral boron sites or interstitials. The 370 nm centre may also be assigned to F^+ colour centre. It is possible, moreover, that the 225 and 370 nm centres are perturbed V_k centres arising due to the lithium vacancy pair presence. So, after γ-irradiation of $Li_2B_4O_7$:Mn crystal, one can observe many radiation-induced centres and the simultaneous presence of different manganese ions of different symmetries that may interact each other [8]. The results were confirmed by EPR measurements presented elsewhere [17].

The presence of Mn^{2+} ions in the LBO:Mn crystal was confirmed mainly by RL measurements. As one can see from Fig. 4, clear 430 (blue) and 610 nm (red) emission bands are observed, suggesting the presence of some types of excitons in the crystal and Mn^{2+} ions, respectively. Moreover, some other type of emission is observed for wavelengths higher than 700 nm. We assign them to Mn^{4+} and Mn^{3+} ion emissions [18]. From Fig. 4 one can also see the dependence of the ratio of intensities $I(G_1)/I(G_2)$ of blue emission band on temperature. We found the ratio
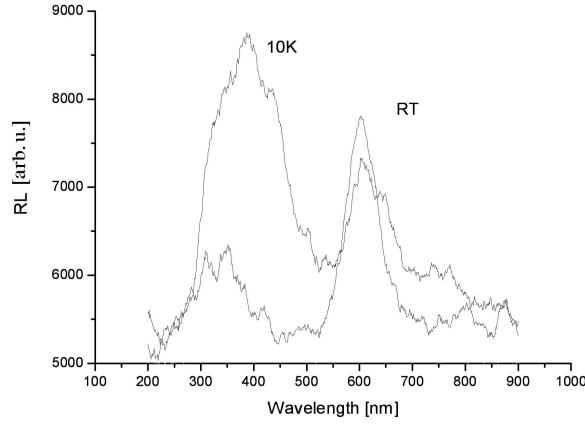
Fig. 4. The radioluminescence spectrum of LBO:Mn single crystal at RT and 10 K.

also depends on other factors, as e.g. crystallographic orientation of a sample. As one can see from the figure the relative intensity of the "red" and "blue" emissions depends on temperature.

Low temperature TL measurements performed for LBO:Mn crystals (see Fig. 6) have revealed a rich TL spectrum with characteristic, extremely narrow peaks that give evidence of the piezoelectric nature of LBO:Mn single crystal (see values of steady state RL). In the temperature range from 10 to 310 K we can distinguish, moreover, at least five TL peaks at about 95, 110, 130, 165, and 215 K that can be assigned to some types of traps (electron and hole types) present inside the bandgap of our crystal. The TL glow curves were fitted, using the classic 1st order equation based on the Randall–Wilkins model [19] and the procedure described in detail by Drozdowski et al. [20]. The trap parameters, i.e. the depths E and frequency factors s, derived from the fitting procedure, are summarized in Table I. As one can see the results characterise four shallow traps of the depths $E = 0.1-0.2$ eV. We can assign them to F$^+$ and/or Mn^{0}B, V_k and

TABLE I

The traps parameters detected in thermoluminescence of Li$_2$B$_4$O$_7$:Mn (n_0 — initial concentration of centres; E — activation energy; s — frequency factors).

Peak number	n_0 [arb. units]	E [eV]	$\ln(s)$
1	2.120×10^5	0.043	0.88
2	1.045×10^4	0.154	11.89
3	2.379×10^4	0.123	6.57
4	2.506×10^4	0.240	12.45

Mn^{3+}, Mn^{6+} centres [18]. The higher TL peak registered at about 100 K may be attributed to F^+ colour centre.

From Fig. 5 it results, moreover, the ratio of the intensities: TL/(steady-state + TL) = 0.6, so only about 40% of all the radiation-induced centres recombine thus after X-ray irradiation, while about 60% of the centres are initially trapped.
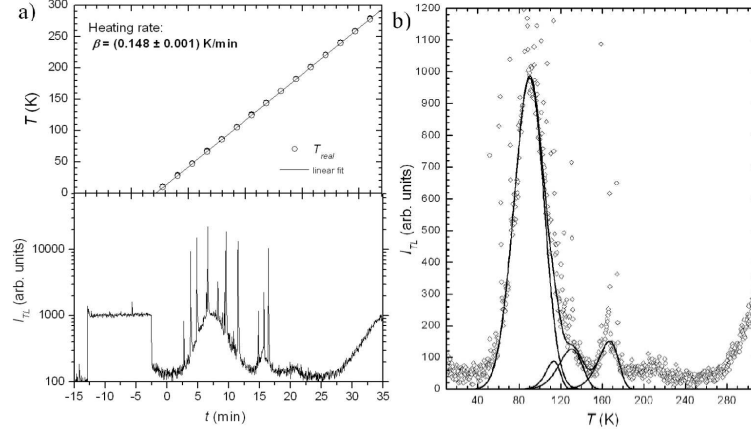

Fig. 5.   The temperature dependence and the steady-state RL (a), the X-ray TL curve and 1st order fit for LBO:Mn single crystals (b).
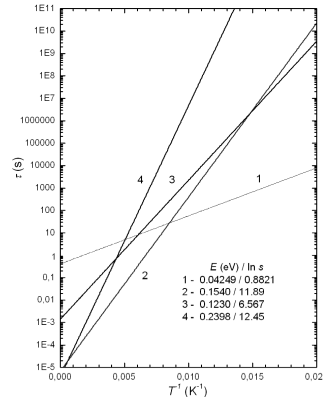

Fig. 6.   The Arrhenius plot of the temperature dependences of the decay times of the X-ray induced changes in the LBO:Mn "as-grown" crystal.

In Fig. 6 we have shown the dependence of the lifetimes, τ, of the four traps as a function of a reverse temperature T. The curves were calculated according to the following Arrhenius formula:

$$\tau^{-1} = \tau_0^{-1} \exp(-\Delta E/k_{\mathrm{B}}T), \tag{2}$$

where ΔE is the activation energy and k_{B} is the Boltzmann constant.
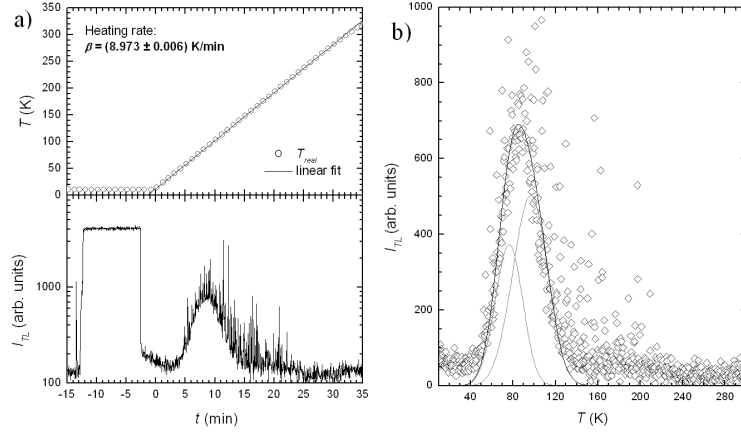
Fig. 7. Temperature dependence and the steady-state RL (a), the X-ray TL curve and 1st order fit for LBO pure single crystals (b).
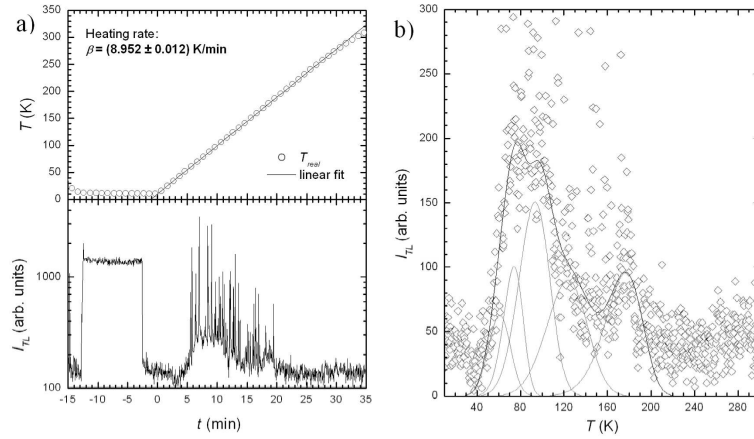

Fig. 8. Temperature dependence and the steady-state RL (a), the X-ray TL curve and 1st order fit for LBO:Yb single crystals (b).

We performed similar investigations for pure LBO (Fig. 7), LBO doped with Yb (Fig. 8) and LBO doped with Co (Fig. 9).

In case of pure LBO, in the temperature range from 10 to 310 K, we can distinguish only two TL peaks at about 95 and 110 K that can be assigned to the same types of traps (electron and hole types) present inside the bandgap of the crystal as in case of LBO:Mn crystal. The trap parameters, i.e. the depths E and frequency factors s, derived from the fitting procedure, are summarized in Table II. As one can see the results characterise two shallow traps of the depths $E \sim 0.1$ eV. We assign them to F-type centres that may respond to the double absorption band registered for the LBO:Mn crystal after γ-irradiation at about 227 nm.
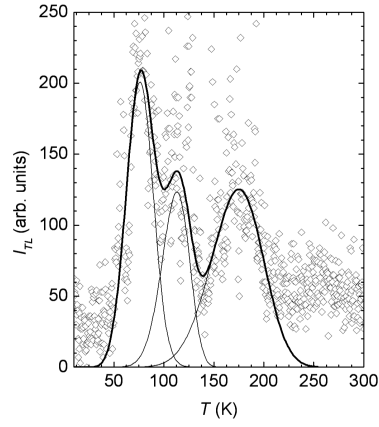
Fig. 9. The glow curves of LBO:Co single crystals, following a 10 min X-ray irradiation.

TABLE II

The initial concentrations, n_0, activation energies, E [eV], and, frequency factors, s, of two traps occurring in the LBO single crystal, derived from the first-order glow curve fits.

Peak number	n_0 [arb.units]	E [eV]	$\ln(s)$
1	7.055×10^4	0.0338	0.648
2	1.202×10^5	0.0429	0.433

In case of LBO:Yb in the temperature range from 10 to 310 K we can distinguish at least five TL peaks at about 60, 75, 95, 130, and 180. The trap parameters, i.e. the depths E and frequency factors s, derived from the fitting procedure, are summarized in Table III. As one can see the results characterise five shallow traps of the depths $E = 0.1-0.2$ eV.

TABLE III

The initial concentrations, n_0, activation energies, E [eV], and, frequency factors, s, of five traps occurring in the LBO:Yb single crystal, derived from the first-order glow curve fits.

Peak number	n_0 [arb.units]	E [eV]	$\ln(s)$
1	9.379×10^3	0.0276	1.017
2	1.442×10^4	0.0475	3.273
3	3.242×10^4	0.0468	1.213
4	2.547×10^4	0.0625	0.997
5	2.696×10^4	0.1450	4.717

We observed a very similar pattern for LBO:Co single crystals (Fig. 9).

Comparing all the TL results one can conclude: there are some types of shallower traps one can distinguish in all measured crystals assigned to point defects (F-type) in pure LBO crystal and dipper additional one characteristic of specific dopant.

4. Conclusions

The pure and Mn-doped crystals were found to be highly transparent, and clear. The Co-doped crystals were purple-blue in colour, transparent, and clear. The crystals grown with Yb_2O_3 had a lot of segregated phases with little transparency.

Mainly Co-doped LBO crystal reveals clear absorption bands near 500 nm and 1100 nm being electronic transitions characteristic of Co^{2+} ions. The crystal is anisotropic, so different shapes of the absorption bands are registered for different sample orientations. In the absorption spectrum of LBO:Yb crystals we have not observed Yb^{3+} transitions but some other UV bands suggest Yb^{2+} substitution.

Irradiation with γ quanta does not change the structure of the absorption. In the absorption spectrum of LBO:Mn crystal the Mn^{2+} absorption band is not observed. So, LBO:Mn "as-grown" crystal does not show photoemission bands coming from Mn^{2+} ions. This is due to a low manganese concentration and due to the low oscillator strength of its $d-d$ absorption transitions. But RL spectra reveal wide blue and red emission bands suggesting the presence in the crystal some excitons and Mn^{2+} ions. Some additional absorption bands are observed in the LBO:Mn crystals under the influence of γ-ray irradiation (Mn^{2+}, Mn^{3+}, Mn^{6+}). The results of TL measurements suggest that in the LBO:Mn crystal the Mn^{1+} ions are present.

Low temperature TL measurements have revealed a rich TL spectrum with characteristic narrow peaks that give evidence of the piezoelectric nature of LBO single crystal, both pure and doped with Yb, Mn and Co. In the temperature range from 10 to 310 K we distinguished, moreover, at least two TL peaks that are associated with some types of electron traps present inside the bandgap of our crystal. The energy depths as high as 0.1–0.2 eV and concentrations of the traps were calculated using Randall–Wilkins procedure. The higher TL peak registered at about 95 K may be attributed to F-type colour centre. We assigned the origin of other peaks to dopant with different valence states.

Acknowledgments

References

[1] D.S. Robertson, I.M. Young, *J. Mater. Sci.* **17**, 1729 (1982).

[2] S.J. Fan, W. Wang, J.J. Xiang, J.K. Xu, *J. Cryst. Growth* **99**, 811 (1990).

[3] R.W. Whatmore, N.M. Sharrocks, C.O. Hara, F.W. Ainger, I.W. Young, *Electron. Lett.* **17**, 11 (1981).

[4] Ya.V. Burak, B.V. Padlyak, V.M. Shevel, *Nucl. Instrum. Methods Phys. Res. B* **191**, 633 (2002).

[5] U. Lanver, G. Lehmann, *J. Lumin.* **17**, 225 (1978).

[6] J. Ramirez-Serrano, E. Madrigal, F. Ramos, G.U. Caldino, *J. Lumin.* **71**, 169 (1997).

[7] N. Senguttuvan, M. Ishii, M. Shimoyama, M. Kobayashi, N. Tsutsui, M. Nikl, M. Dusek, H.M. Shimizu, T. Oku, T. Adachi, K. Sakai, J. Suzuki, *Nucl. Instrum. Methods Phys. Res. A* **486**, 264 (2002).

[8] B. Henderson, G.F. Imbush, *Optical Interaction of Inorganic Solids*, Clarendon Press, Oxford 1989.

[9] Kang-Soo Park, J.K. Ahn, D.J. Kim, H.K. Kim, Y.H. Hwang, D.S. Kim, M.H. Park, Yumi Park, Jin-Joo Yoon, Jae-Young Leem, *J. Cryst. Growth* **249**, 483 (2003).

[10] I.N. Ogorodnikov, V.A. Pustovarov, L.I. Isaenko, E.I. Zinin, A.V. Kruzhalov, *Nucl. Instrum. Methods Phys. Res. A* **448**, 467 (2000).

[11] V. Skvortsova, N. Mironova-Ulmane, U. Ulmanis, A. Matkovskii, *Nucl. Instrum. Methods Phys. Res. B* **166-167**, 284 (2000).

[12] G.U. Caldino, O.J. Rubio, *Radiat. Eff. Defects Solids* **127**, 83 (1993).

[13] R. Clause, K. Petermann, *IEEE, J. Quantum Electron.* **24**, 1114 (1988).

[14] B. Chandra, R.C. Bhatt, *Instrum. Methods* **184**, 557 (1981).

[15] Ya.V. Burak, B.V. Padlyak, V.M. Shevel, *Nucl. Instrum. Methods Phys. Res. B* **191**, 633 (2002).

[16] V.T. Adamiv, Ya.V. Burak, I.V. Kityk, J. Kasperczyk, R. Smok, M. Czerwiński, *Opt. Mat.* **8**, 207 (1997).

[17] D. Podgórska, S.M. Kaczmarek, M. Wabia, M. Kwaśny, S. Warchoł, *Mol. Phys. Rep.* **39**, 199 (2004).

[18] G.B. Loutts, M. Warren, L. Taylor, R.R. Rakhimov, H.R. Ries, G. Miller, *Phys. Rev. B* **57**, 3706 (1998).

[19] J.T. Randall, M.H.F. Wilkins, *Proc. R. Soc. Lond. A* **184**, 366 (1945).

[20] W. Drozdowski, K.R. Przegiętka, A.J. Wojtowicz, H.L. Oczkowski, *Acta Phys. Pol. A* **95**, 251 (1999).